Global and Planetary Change 173 (2019) 73–82

Contents lists available at ScienceDirect

Global and Planetary Change

journal homepage: www.elsevier.com/locate/gloplacha

Invited research article

Snow depth reconstruction over last century: Trend and distribution in the Tianshan Mountains, China

Qian Li[a,b], Tao Yang[a,b], Feiyun Zhang[c], Zhiming Qi[a], Lanhai Li[a,d,e,f,*]

[a] State Key Laboratory of Desert and Oasis Ecology, Xinjiang Institute of Ecology and Geography, Chinese Academy of Sciences, Urumqi 830011, China
[b] University of Chinese Academy of Sciences, Beijing 100049, China
[c] Faculty of Management, Xinjiang Agricultural University, Urumqi 830052, China
[d] Ili Station for Watershed Ecosystem Research, Chinese Academy of Sciences, Xinjiang 830011, China
[e] CAS Research Center for Ecology and Environment in Central Asia, Xinjiang 830011, China
[f] Xinjiang Regional Center of Resources and Environmental Science Instrument, Chinese Academy of Sciences, Urumqi 830011, China

ARTICLE INFO

Keywords:
Historical snow depth reconstruction
Tianshan Mountains
Artificial neural networks method
Reanalysis data
Climate change

ABSTRACT

Clarifying the long-term variations in snow depth is important for hydrological, meteorological and ecological implications. However, the short period of snow depth records in the mountains has made the assessment of regional long-term variation of snow depth difficult. Based on reanalysis datasets from 1901 to 2014 as well as observational data from 1961 to 2014, this study applied the artificial neural networks (ANN) method to reconstruct the historical snow depths in the Tianshan Mountains of China from 1901 to 1960. The variations in monthly snow depth were analyzed during the periods of 1901–1960, 1961–2014, and 1901–2014 as historical, observed, and overall periods, respectively. The results indicated that the reconstructed snow depths captured the long-term variation and spatial distribution in the study area. For temporal scale, increases in snow depth were detected in the southern and eastern Tianshan Mountains during all three periods. The trends in snow depth indicated an increase in the western, northern and overall Tianshan Mountains during the periods of 1901–1960 and 1961–2014, but showed a decrease during the overall period of 1901–2014. The difference in variation of snow depth trends in different temporal scales indicates that the time scale of snow depth increase is decadal rather than centennial. For spatial scale, higher values of snow depth occurred in the western and northern Tianshan Mountains, while lower ones appeared in the southern and eastern Tianshan Mountains. In addition, the increasing trend in the reconstructed snow depth was more profound with increased elevation in the Tianshan Mountains during 1901–1960, with the smallest increasing rate at the elevation of 1000 m–1500 m. Although some uncertainties exist within the reconstruction, this work proposed a method for developing historical snow depth for observation-limited areas, which provided additional data for hydrological and ecological simulation. The results also allow us to achieve a better understanding of regional climate change.

1. Introduction

As a good indicator reflecting climate change, snow has experienced a series of changes from regional to hemispheric scales over recent decades with different trends. Snow cover duration shortened over southern Siberia, Eurasia, Central Asia and northwestern China, but snow accumulation during winter has increased in these regions (Bulygina et al., 2011; Ma and Qin, 2012; Qin et al., 2006; Ye and Ellison, 2003; Zhou et al., 2017). In addition, downward trends in snow depth and snow cover duration were found in North America and the Qinghai-Tibetan Plateau (Dyer and Mote, 2006; Xu et al., 2017). As a result, the response of snow to climate change could vary at different spatiotemporal scales. Moreover, seasonal snowmelt provides a runoff supply which substantially contributes to freshwater resources (Aizen et al., 1995), and causes droughts or floods, especially in arid regions (Zhang et al., 2016a). Under the background of global warming, earlier snowmelt was expected to occur in winter and early spring, which would substantially affect the ecosystem and water availability in snow-dominated regions (Barnett et al., 2005). Therefore, effectively monitoring snow is not only helpful for the assessment of climate change, but is also essential for water resource management and environmental protection. However, it is still a challenge to assess the long-term

* Corresponding author at: State Key Laboratory of Desert and Oasis Ecology, Xinjiang Institute of Ecology and Geography, Chinese Academy of Sciences, Urumqi 830011, China.
E-mail address: lilh@ms.xjb.ac.cn (L. Li).

https://doi.org/10.1016/j.gloplacha.2018.12.008
Received 26 July 2018; Received in revised form 12 December 2018; Accepted 18 December 2018
Available online 19 December 2018
0921-8181/ © 2018 Elsevier B.V. All rights reserved.

variation of snow depth under climate change, because of the short observation period of *in-situ* records and remote sensing retrieval data, as well as the accuracy of remote sensing data.

The simulations from the global circulation model (GCM) and the regional climate model (RCM), as well as reanalysis fields have been used in climatic and hydrological studies for the need of long-term data series. Some studies used RCM simulations and reanalysis data to project the future climate data (Hagemann et al., 2011; Lenderink et al., 2007; Teutschbein and Seibert, 2012; Li et al., 2013; Reyers et al., 2013), and then projected future streamflow (Chen et al., 2011; Johnson and Sharma, 2011), showing the potential of using RCM simulations and reanalysis fields for long-term climatic and hydrological applications. However, bias often existed in these data compared with direct observations due to varying spatial and temporal resolutions, making bias correction necessary (Christensen et al., 2008; Teutschbein and Seibert, 2012). After bias correction, reconstructed and projected climate fields can be used to estimate the streamflow in data scarce regions (Li et al., 2013; Zhang et al., 2016b). However, studies applying climate data to reconstruct the historical snow depths are still rare.

The accumulation and ablation process of snowpack are complex processes due to the integrated influence of meteorological factors, such as temperature, precipitation, wind speed, humidity and so on. Precipitation positively influences snow depth in the cold season, while temperature plays a major role in affecting trend and variability of snow depth over time (Barnett et al., 2005; Li and Simonovic, 2002). Qin et al. (2006) and Brown et al. (2010) found that there exists a correlation between snow depth and meteorological factors, which can be interpreted by linear regression analysis. Compared with the linear regression method, artificial neural networks (ANN) prevail in non-linear approaches, and have been widely employed for predictions in hydrological and climate studies (Hsu and Gupta, 1995; Imrie et al., 2000; Moghim and Bras, 2017). The ANN method can provide accurate results in snow depth and snow water equivalent simulations (Tedesco et al., 2004), as well as snow parameters retrieval from remote sensing data (Dobreva and Klein, 2011; Tedesco et al., 2004). Hence, the ANN method has the potential for interpreting snow depth dynamics because it is flexible enough to deal with non-linear processes.

The Tianshan Mountains are located in Central Asia, with the eastern part in Xinjiang, China. As an important water resource of this region, the Tianshan Mountains of China contribute about 9.63×10^9 m^3 to the annual runoff by snowmelt and ice melt (Hu, 2004). Water vapor sources, climatic conditions and topographic complexity result in a great difference in the spatiotemporal distribution of snowfall regimes (Guo and Li, 2015), which further leads to the varied distribution of snow depth. Although a remarkable increasing trend in snow depth has been detected over the entire mountain (Dou and Chen, 2010), studies concerning the different responses of snow depth to climate change within the Tianshan Mountains are still insufficient. In addition, the short period of snow depth records limits studies on climate change assessment, as well as the evaluation of regional hydrological models and land surface models, because the meteorological stations were mostly set up in the late 1950s in the Tianshan Mountains, China. Hence, historical snow depth reconstruction is necessary in order to better understand the long-term spatiotemporal variation and distribution of snow depth in the Tianshan Mountains, China.

Based on both reanalysis dataset from 1901 to 2014 and observed records from 1961 to 2014, this study applied the ANN method to reconstruct the historical snow depths from 1901 to 1960 for the Tianshan Mountains region where long-term observations are lacking. The objectives of this study are to: (1) reconstruct the daily snow depth series in the Tianshan Mountains from 1901 to 1960, (2) clarify the variation of snow depth with different periods during the historical period (1901–1960), observed period (1961–2014), and the overall period (1901–2014) by analyzing monthly mean snow depth. The results of this study could provide information to obtain a better understanding of regional climate change, and assist with comparison and evaluation for model simulation and future projection.

2. Data and method

2.1. Study area

The Tianshan Mountains in Xinjiang, China are located at 34.34°–55.43°N and 75°–96.37°E. The topographical and geomorphological patterns of study area are characterized by glaciers, forests, shrubs, grasslands, croplands, and widespread deserts (Hu, 2004). The winter mean temperature is −10–-18.3 °C on the northern slope and − 2.3–-12.2 °C on the southern slope. The mean annual precipitation is over 200 mm on the northern slope of the Tianshan Mountains, while only 50–100 mm on the southern slope. The annual maximum precipitation can reach 350–550 mm in the Yili River Valley which is located in the western Tianshan Mountains, but only 10–30 mm is in the eastern part, which is the minimum precipitation of the entire Tianshan Mountains (Xu et al., 2018). Similar to the distribution of precipitation, snow depth also decreases from west to east, and from north to south. Forty-eight meteorological stations with geo-coordinates (Table 1) are shown in Fig. 1, as well as their mean snow depth during winter. Stations in the Yili River Basin are located in elevations ranging from 321.2 m to 1854.6 m with snow depths from 1.4 cm to 18.2 cm, while the stations in the northern part are situated from 347.8 m to 3543.8 m with snow depths from 4.1 cm to 22.4 cm. The mean daily snow depth in winter was much lower in the eastern part with 1.9 cm and in the southern part with 1.3 cm (Qiu and Sun, 1992).

2.2. Data

Based on the continuity of data, daily temperature, precipitation, and snow depth from 48 meteorological stations during the period of 1961–2014 were chosen from China Meteorological dataset version 3.0 (http://data.cma.cn/site/index.html) for this study. The dataset was reliable with strict quality control. The NOAA-CIRES 20th century reanalysis (V2c) provides a four-dimensional global atmospheric dataset at 2.0° resolution of the entire 20th century for climatological and hydrological studies (Compo et al., 2011). Daily precipitation was a total from eight time levels each day, while daily temperature was the mean value from four time levels each day. Daily precipitation and temperature fields from the reanalysis dataset, which were selected from the period of July 1901 to December 2014, were then re-sampled to the station scale.

Firstly, the observed daily temperature and precipitation were used to evaluate the errors between the raw reanalysis data and the observations during 1961–2014, which was then used to correct the bias of the raw reanalysis data during 1901–2014. Secondly, the observed daily temperature, precipitation, and snow depth were used to calibrate and validate the six structures of ANN networks for each station (Table 2). Furthermore, the corrected reanalysis temperature and precipitation during 1901–2014 were used as inputs for snow depth reconstruction in terms of best structured networks for each station. Based on the results from snow depth reconstruction, the reconstructed snow depth during 1961–2014 was applied for evaluation with observations; the reconstructed snow depth during 1901–1960 was used for the analysis of historical variation and distribution of snow depth; and the combined snow depth series from reconstructed historical data and observation data were used for assessing long term variation and distribution of snow depth.

2.3. Method

2.3.1. Artificial neural networks

The change within snowpack is a complex physical process. For

Table 1
Station information.

Name	Station	Lon.	Lat.	Altitude	Name	Station	Lon.	Lat.	Altitude
Alashankou	51232	82.57	45.18	338.1	Tianchi	51470	88.12	43.88	1935.2
Bole	51238	82.07	44.90	532.9	Dabancheng	51477	88.32	43.35	1105.3
Khorgas	51328	80.42	44.20	774	Shisanjianfang	51495	91.73	43.22	792
Wenquan	51330	81.02	44.97	1353.9	Bayanbulak	51542	84.15	43.03	2458.9
Jinghe	51334	82.90	44.60	321.2	Hejing	51559	86.40	42.32	1110.3
Usu	51346	84.67	44.43	478.3	Yanqi	51567	86.57	42.08	1057.9
mosuowan	51353	86.10	45.02	347.8	Shanshan	51581	90.23	42.85	399.1
Shihezi	51356	86.05	44.32	444.1	Wushi	51627	79.23	41.22	1396.8
Manasi	51359	86.20	44.32	473.1	Aksu	51628	80.23	41.17	1105.4
Caijiahu	51365	87.53	44.20	441	Baicheng	51633	81.90	41.78	1230.4
Hutubi	51367	86.82	44.13	523.5	Xinhe	51636	82.62	41.53	1014.5
Jimusaer	51378	89.17	44.02	735.8	Shaya	51639	82.78	41.23	981.5
Qitai	51379	89.57	44.02	794.3	Kuche	51644	82.97	41.72	1082.9
Chabuchaer	51430	81.15	43.83	603.6	Torugart	51701	75.40	40.52	3507.4
Yining	51431	81.33	43.95	663.4	Wuqia	51705	75.25	39.72	2177.5
Nileke	51433	82.52	43.80	1106.1	Jiashi	51707	76.73	39.50	1210.9
Gongliu	51435	82.23	43.47	776.5	Kashgar	51709	75.98	39.47	1291.3
Xinyuan	51436	83.30	43.45	929.2	Akqi	51711	78.45	40.93	1986
Zhaosu	51437	81.13	43.15	1854.6	Bachu	51716	78.57	39.80	1117.6
Tekesi	51438	81.77	43.18	1210.9	Kalpin	51720	79.05	40.50	1163
Urumqi	51463	87.61	43.83	935.9	Aral	51730	81.27	40.55	1013
Xiaoquzi	51465	87.10	43.48	2121.2	Balikun	52101	93.05	43.60	1650.9
Balguntay	51467	86.32	42.73	1739.7	Yiwu	52118	94.70	43.27	1729.5
Daxigou	51468	86.83	43.10	3543.8	Hami	52203	93.52	42.82	738.8

instance, the interior melting water within snowpack could refreeze, due to the diurnal temperature above 0 °C and the nightly temperature below 0 °C during snowmelt season. These changes are non-linear, which can be modeled by the ANN method. According to a previous study, a three-layer feed-forward network using sigmoid transfer functions can fit multi-dimensional mapping problems arbitrarily well (Hsu and Gupta, 1995). In this study, the ANN models were based on the function of the change in snow depth on the present day and the day prior ($f(x) = xn - 1 + \Delta x$), while temperature and precipitation were the variables that cause the change (Δx) of snow depth in current day and the day before. Six three-layer feed-forward network models with different input variables were trained with Levenberg-Marquardt backpropagation for each station (Table 2). The ANN models had one input layer, one hidden layer, and one output layer. The neuron in input layer contained temperature and precipitation at times n, n-1, and n-2, and snow depth at time n-1, while the only neuron in output layer was snow depth at time n, building the network by adding one hidden neuron in the hidden layer at a time (see Fig. 2). To accomplish the calibration and validation phases of ANN models, the input for each station was automatically and randomly divided into three datasets: 70% for training, 15% for validation, and 15% for testing. The training set was used for training the networks, while validation set was used to validate the generalization of networks and to stop training before overfitting. During and after training, the independent inputs in the testing set were used to test the generalization of networks. Then, the

Table 2
Structures of the ANN networks.

Numbers of inputs	Variables of input	Variables of output	Type
3	T_n, P_n, and S_{n-1}	S_n	I1
5	T_n, P_n, T_{n-1}, P_{n-1}, and S_{n-1}	S_n	I2
4	T_n, T_{n-1}, P_n, and S_{n-1}	S_n	II1
5	T_n, T_{n-1}, T_{n-2}, P_n, and S_{n-1}	S_n	II2
4	T_n, P_n, P_{n-1}, and S_{n-1}	S_n	III1
5	T_n, P_n, P_{n-1}, P_{n-2}, and S_{n-1}	S_n	III2

Notes: T represents temperature, P represents precipitation, and S is snow depth. Subscript n means the variables were in the day n, n-1 means one day before, and n-2 means two days before.

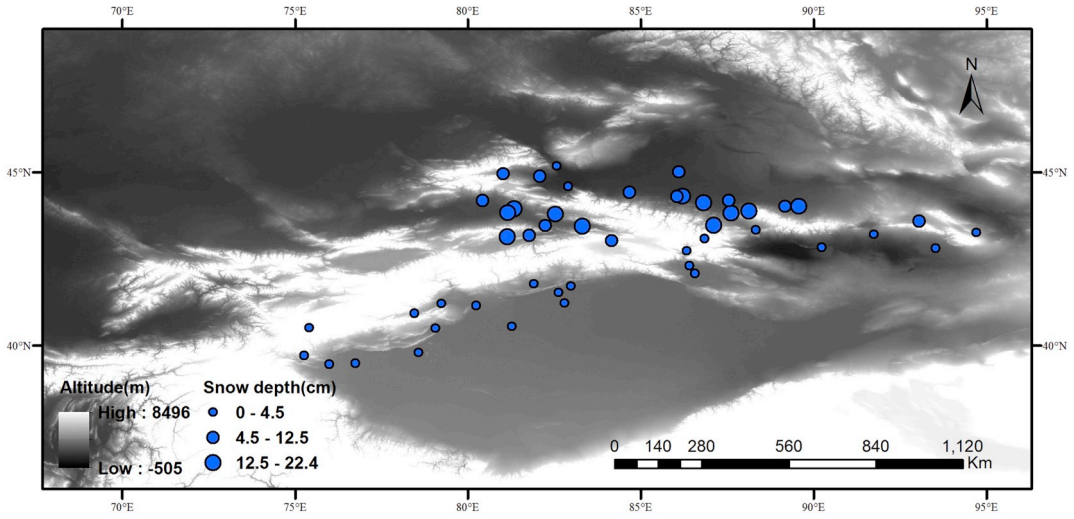

Fig. 1. Study area with meteorological stations. The size of circle represents the mean snow depth during winter at each station from1961 to 2014.

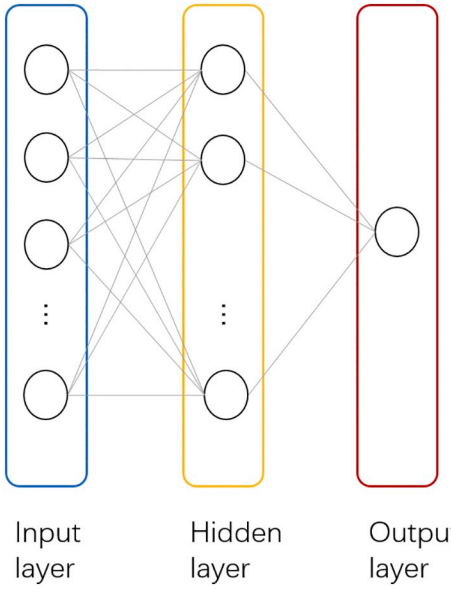

Fig. 2. Schematic diagram of three-layered ANN models in this study.

best structured ANN model was selected out of six ANN models for each station by comparing correlation coefficient (R value), bias, and root mean square error (RMSE) between the model outputs and observations.

2.3.2. Correction of reanalysis dataset

Bias correction methods include linear scaling, local intensity scaling, power transformation, variance scaling, and distribution transfer. Chen et al. (2016) found that all bias correction methods performed similarly after modeling hydrological simulations. Correcting the precipitation field is more difficult than that of the temperature field because of its spatiotemporal variability and nonlinearity (Lenderink et al., 2007). In this study, the correction factor and addends were assumed to be the same before 1960 and after 1960 throughout the reanalysis data. For temperature, the linear scaling method is used (Lenderink et al., 2007):

$$T(d) = Treana(d) + \mu m(Tobs(d)) - \mu m(Treana(d)) \quad (1)$$

Where μm is monthly mean of observations, and $Tobs(d)$ and $Treana(d)$ are daily temperature series from observations and reanalysis, respectively.

According to the local intensity scaling method (Schmidli et al., 2006; Widmann et al., 2003), a downscaled precipitation series was obtained by calibrating a scaling factor at the daily scale. The downscaled precipitation had the same wet-day frequency (FRE) and intensity (INT) as *in-situ* observations. The local intensity scaling could compensate for GCM's errors by monthly or seasonal basis calibration (Schmidli et al., 2006). The local intensity scaling method consists of two steps. First, determining a wet-day threshold $P_{WDT}{}^{reana}$ from the daily reanalysis precipitation series, rendering the threshold exceedance matching the FRE in the observed series; second, based on the same INTs between observations and reanalysis data, a scaling factor S, which adjusts the reanalysis data, is calculated by:

$$S = \frac{\mu_{sea}(P^{obs}: P^{obs} \geq P^{obs}_{WDT}) - P^{obs}_{WDT}}{\mu_{sea}(P^{reana}: P^{reana} \geq P^{reana}_{WDT}) - P^{reana}_{WDT}} \quad (2)$$

Where P^{obs} and P^{reana} are daily precipitation values of the observations and the reanalysis dataset, respectively. $P_{WDT}{}^{obs}$ is days with precipitation ≥ 1 mm, which is the wet-day threshold for *in-situ* observations. μ_{sea} expresses seasonal averages. Finally, the daily precipitation series P is adjusted by S and obtained by:

Table 3
Performance of NOAA-CIRES dataset against observations during 1961–2014.

	Raw data		Corrected data	
	Temperature (°C)	Precipitation (mm)	Temperature (°C)	Precipitation (mm)
Bias	4.9	8.0	0.02	1.0
RMSE	7.2	15.1	0.09	1.5

$$P(d) = \begin{cases} 0, & \text{if } P^{reana}(d) < P^{reana}_{WDT} \\ P^{reana}(d) \cdot S, & \text{otherwise} \end{cases} \quad (3)$$

3. Results

3.1. Evaluation of raw and corrected reanalysis data

Table 3 shows the performance of the raw and corrected daily temperature as well as the precipitation from the reanalysis dataset against *in-situ* observations during 1961 to 2014. Bias and root mean square error (RMSE) were chosen as metrics for evaluation. The ensemble mean bias and RMSE of raw temperature against *in-situ* observations were 4.9 °C and 7.2 °C, respectively. The temperature from the reanalysis data showed warm bias at most stations, especially in winter and summer, but cold bias in spring and autumn. The ensemble mean bias of raw precipitation was 8.0 mm and the RMSE was 15.1 mm. The reanalysis data were wetter than observations at almost every station, with the highest wet bias in winter but the lowest wet bias in summer. Too many low intensity precipitation events contributed to the overestimation, which occurred in the precipitation field from the raw reanalysis dataset. According to Eqs. (2) and (3), the corrected reanalysis precipitation was calibrated to have the same mean, wet-day frequency, and intensity as the observations. The scaling factors of most stations were below 1, revealing that the reanalysis overestimated precipitation except for those in summer. After correction, there was a sharp decrease in the ensemble mean bias and RMSE of temperature and precipitation (see Table 3).

3.2. Performance of ANN models compared to observations

The ANN models were trained, validated and tested using the observation data from 1961 to 2014, and the performance of the models was evaluated by correlation coefficient (R), bias, and RMSE. The R value, bias, and RMSE during training, validation, and testing processes are shown in Fig. 3. The ensemble mean R value, bias, and RMSE were 0.969/0.971/0.967, 0.015/0.012/0.018, and 0.686/0.663/0.728 during training, validation, and testing processes, respectively. The model structures with the best performance of each station are shown in Table 4. The results of 13 stations fitted the observed snow depths better, with only T_n and P_n as inputs. The ANN models containing T_{n-1} or T_{n-2} as inputs performed better in 14 stations which were widely distributed throughout the southern and eastern section of the Tianshan Mountains (see Table 4). However, 10 stations with the best performance simulated with P_{n-1} or P_{n-2} as inputs were mainly located in the Yili River Valley and the middle northern part. The other stations with T_{n-1} and P_{n-1} as inputs for ANN models were mainly distributed in the Yili River Valley, and both the northern and southern of the middle part in the Tianshan Mountains.

3.3. Reconstructed snow depth

The reconstructed snow depth from 1901 to 2014 was obtained by the best structured models with the corrected reanalysis data as inputs. The ensemble monthly mean bias and the RMSE of reconstructed snow depth against observations from 1961 to 2014 were 0.5 cm and 1.7 cm, respectively. The correlation coefficient between the monthly mean

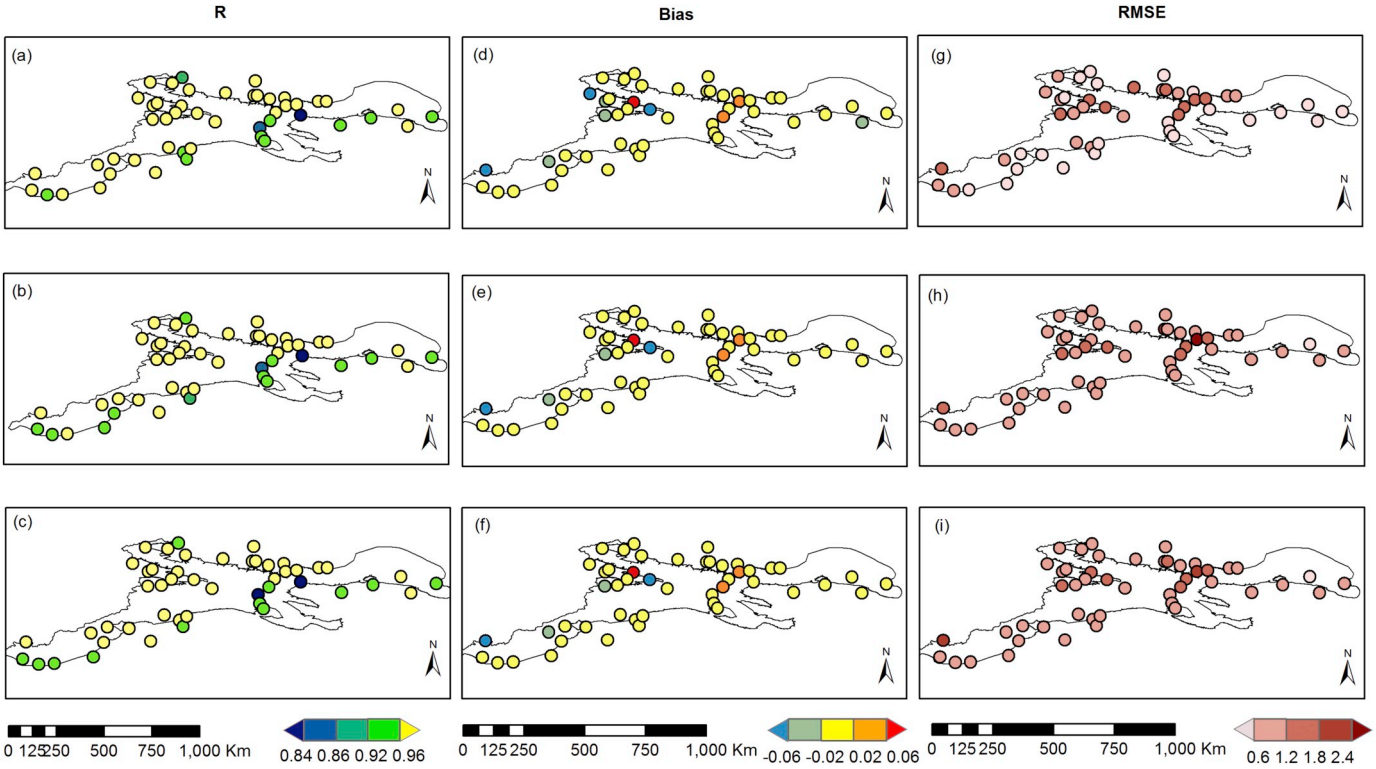

Fig. 3. Performances of ANN method for each station. (a), (d), and (g) indicate the performances during training processes, (b), (e), and (h) are in validation processes, and (c), (f), and (i) are in testing processes, respectively.

reconstructed snow depth and observations was 0.87 (significant at 0.05 level). Large errors occurred at Tianchi station (bias of 2.0 cm) and Torugart station (bias of 1.8 cm). The stations with lower errors were all located below 2000 m. The mean monthly snow depth of reconstructed snow depth and observations from 1961 to 2014, as well as their linear trends in each month are shown in Fig. 4. The monthly means of reconstructed snow depth captured the annual cycle compared with observations, although it overestimated in winter, and underestimated in autumn and spring. In addition, the trends in each month were similar to observations. The positive values indicated that the monthly snow depth increased during 1961–2014. However, trends in March, August, and September were decreasing during 1961–2014.

The distribution of reconstructed snow depth in winter during 1901–1960 is shown in Fig. 5 (a). Similar to the distribution of the observations during 1961–2014, higher snow depth was seen in the western part and the northern Tianshan Mountains with 8.2 cm and 9.1 cm, and the lower ones occurred in the southern and the eastern part with 0.9 cm and 0.3 cm, respectively. Compared with the observations, the monthly mean of reconstructed snow depth was lower in the study area. Fig. 5 (b) shows the long-term variation of reconstructed monthly mean snow depth from October to April during 1901 to 1960 period. The slightly non-significant upward trend of snow depth over the 60 years was found with the deepest snow depth occurring in 1950 in the Tianshan Mountains. Half of the stations (24) exhibited significant trends over the 60 years with the average increasing rate of 0.23 cm decade^{-1}, which reached the significance level of 0.05. The increasing magnitudes were highest in the elevation above 2000 m (0.73 cm decade^{-1}) and the smallest in the elevation of 1000 m–1500 m (0.12 cm decade^{-1}). The changing rates in snow depth from 1901 to 1960 were 0.15 cm decade^{-1}, 0.16 cm decade^{-1}, and 0.72 cm decade^{-1} in below 500 m, 500 m–1000 m, and 1500 m–2000 m, respectively. Snow depth changed insignificantly at elevations below 1000 m.

4. Discussion

4.1. Temporal trends of snow depth during three periods

On the temporal scale, the time series of reconstructed and observed snow depth can be defined into three periods: observed period (1961–2014), historical period (1901–1960), and overall period (1901–2014). The trend of snow depth in the southern and eastern Tianshan Mountains increased during all three periods, respectively. The trend of snow depth decreased during the overall period in the northern, western, and entire Tianshan Mountains, although the trends increased in historical and observed periods, respectively (Fig. 6).

Table 4
Best structures of ANN models for each station.

Model type	Station ID
I1	51330 (6), 41367 (3), 51435 (13), 51437 (3), 51465 (8), 51470 (11), 51477 (11), 51542 (10), 51581 (3), 51627 (6), 51628 (10), 51633 (11), and 51701 (6)
I2	51232 (3), 51334 (3), 51356 (4), 51359 (3), 51430 (6), 51436 (6), 51467 (3), 51468 (10), 51567 (3), and 51636 (8)
II1	41353 (3), 51379 (3), 51707 (9), 51709 (7), 51711 (10), 51716 (12), 51720 (11), and 52101 (7)
II2	51365 (3), 51431 (3), 51495 (9), 51639 (7), 51644 (5), 51730 (5), and 52118 (4)
III1	51346 (3), 51433 (4), 51463 (4), and 51705 (9)
III2	51238 (3), 51328 (4), 51378 (3), 51438 (3), 51559 (4), and 52203 (3)

The bracket behind station ID indicates the hidden neuron in the hidden layer.

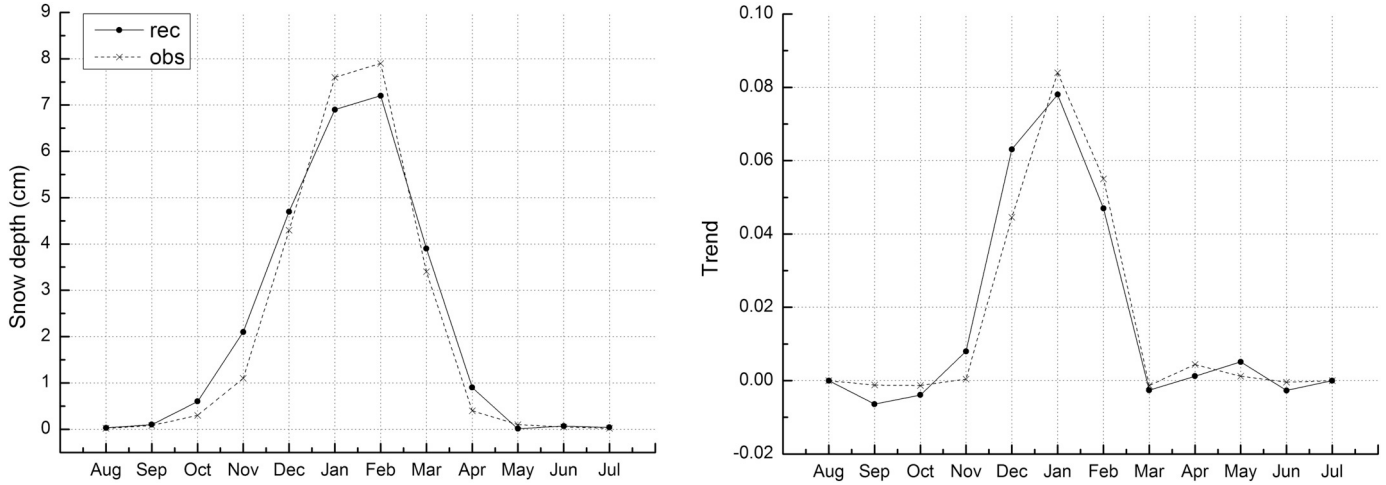

Fig. 4. Mean monthly snow depth (left) and trend (right) of reconstruction and observations, 1961–2014. The trend is the slope of linear trend for each month, the observed data is shown with dashed line and reconstructed data in shown with solid line. The units in x-axis are the abbreviations for each month.

In the historical period, trend analysis showed that the annual temperature and annual precipitation of the entire Tianshan Mountains increased during 1901–1960, only significant at 0.05 confidence level in precipitation (Fig. 7). The trend in snow depth increased but not significant in the entire Tianshan Mountains. This could be due to the significant increased precipitation in the Tianshan Mountains, which was consistent with the overall increase in precipitation over mid-latitude regions of the Northern Hemisphere (Hartmann et al., 2013). In the observed period, the annual precipitation has significantly increased since 1960s in Xinjiang, with the highest increment in winter (Shi et al., 2007; Xu et al., 2018). More water vapor was transported by the strengthened North America Subtropical High and West Pacific Subtropical High to the Tianshan Mountains (Li et al., 2016; Yao et al., 2016), leading to a higher annual precipitation increasing rate in the Tianshan Mountains than that in other parts of Xinjiang (Xu et al., 2018). Consequently, the snow depth also significantly increased in Xinjiang since 1960s (Qin et al., 2006; Yang, 2008). However, a shorter snow cover duration was observed in the Tianshan Mountains due to warmer temperatures in autumn and spring (Tang et al., 2017). Note that the annual precipitation decreased during the 1950s (Fig. 7), which

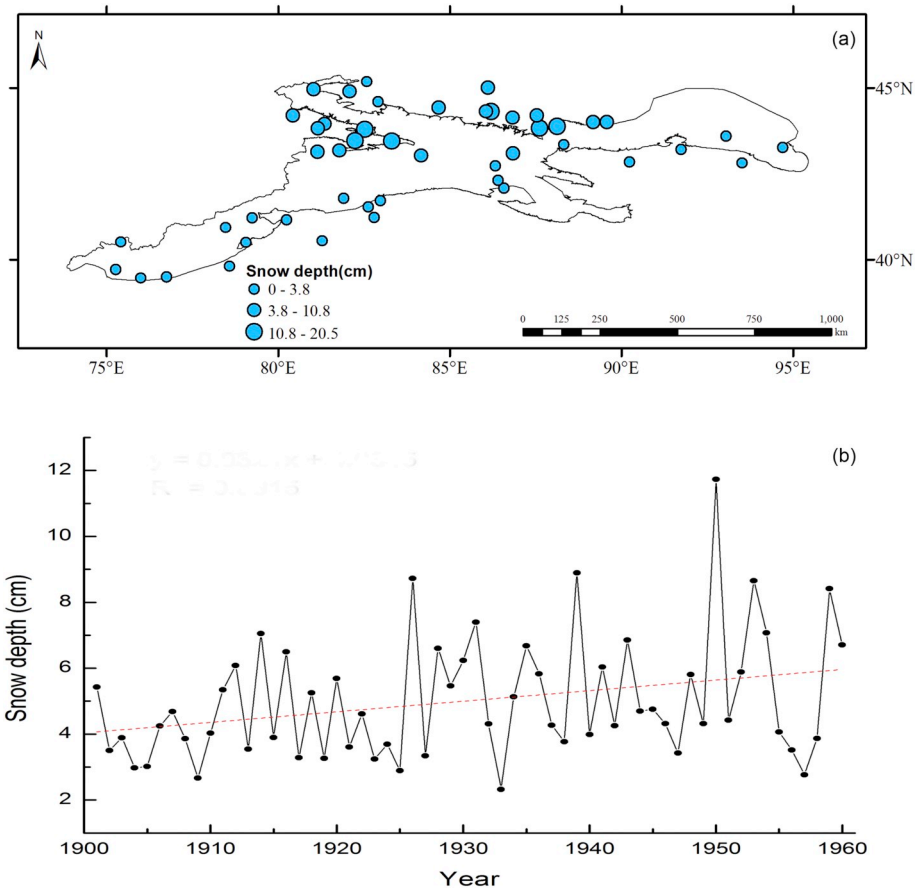

Fig. 5. Distribution (a) and variation (b) of reconstructed snow depth in the Tianshan Mountains during 1901–1960.

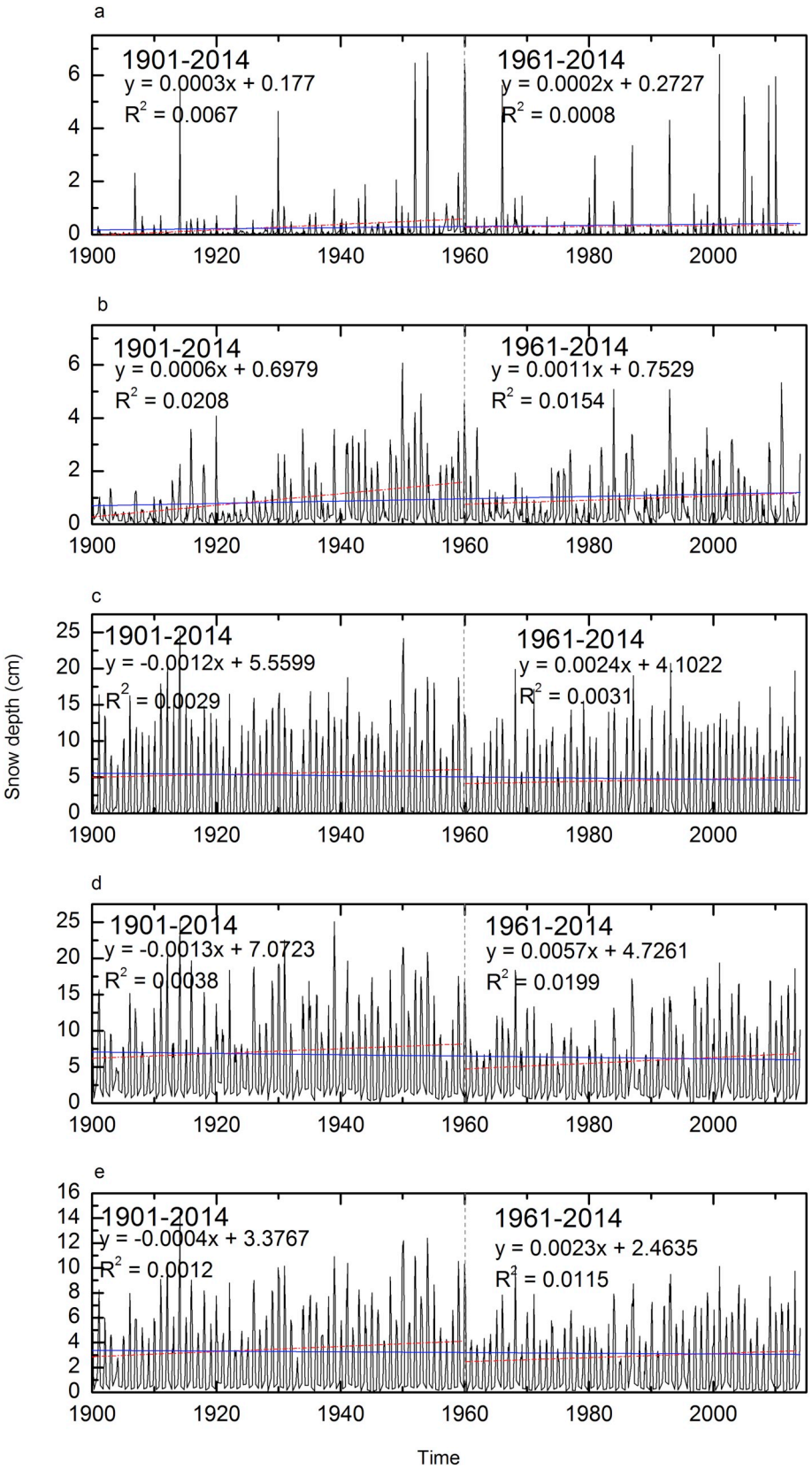

Fig. 6. Different trends of snow depth in the Tianshan Mountains during observed period (1961–2014), historical period (1901–1960), and overall period (1901–2014). A (eastern), b (southern), c (western), d (northern), and e (ensemble mean).

may have caused the increasing trends in snow depth during 1901–1960 and 1961–2014. In the overall period, the snow depth revealed non-significant downward trend in the northern, western, and the whole Tianshan Mountains during 1901–2014. The decline in snow depth during the overall period was coupled with the significant positive trend in temperature since the late 19th century (Hartmann et al.,

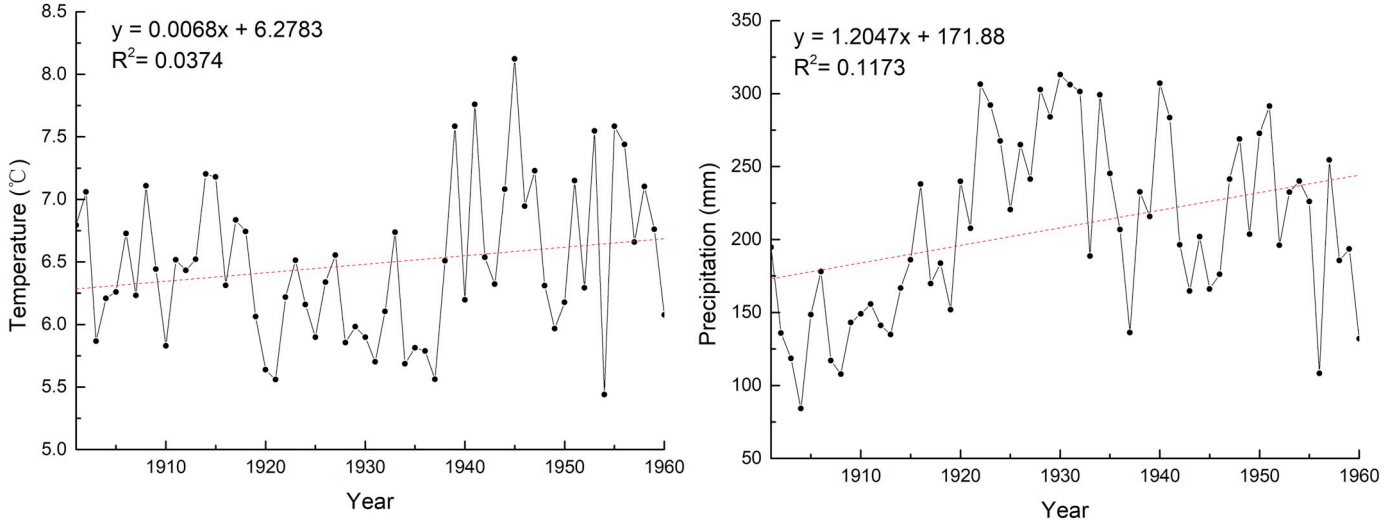

Fig. 7. Trends of annual temperature (left) and annual precipitation (right) in the Tianshan Mountains during historical period (1901–1960).

2013; Li et al., 2013). In addition, although the trend in snow depth slightly increased during the overall period in the southern and eastern Tianshan Mountains, it was not statistically significant due to the shallow snow.

It has been confirmed that trends based on short records are sensitive to the beginning and end dates due to natural variability (Hartmann et al., 2013). Thus, it is important to reconstruct snow depth of the historical period because the trends of snow depth were different during observed, historical, and overall periods in the northern, western, and whole Tianshan Mountains. The different variations of snow depth in different temporal scales indicated that the time scale of snow depth increase is decadal rather than centennial.

4.2. Spatial patterns of reconstructed snow depth

On the spatial scale, the reconstructed snow depth series captured the distribution in different sub-regions, which was in line with the observations and a previous study (Wang et al., 2008). The wind comes from the northwest, and brings out precipitation to the northwest part of Xinjiang (the western Altai Mountains, the Tacheng Basin, and the Yili River Basin). More downdrafts occurred with the weather system pushing southeastwards into the Jungar Basin (Wang et al., 2008). These downdrafts minimally induce precipitation, thus the precipitation decreases from the northwest to the southeast of the study area. The distribution of snow depth mainly depends on the distribution of precipitation. The water moisture carried by the westerly travels through the Yili River Basin into the Tianshan Mountains (Yu et al., 2003; Wei et al., 2005), leading to the largest snow depth which was seen in the western part of Tianshan Mountains (namely Yili River Valley) and the northern Tianshan Mountains. By contrast, less snow was found in the southern and eastern part of the Tianshan Mountains. The finding also revealed an increasing rate of reconstructed snow depth with increasing elevation, with the smallest increasing rate at the elevation of 1000 m–1500 m, implying that the increasing trend of snow depth was amplified with elevation in the Tianshan Mountains during 1901–1960. The smallest increasing magnitude occurred in the elevation of 1000 m–1500 m may be casued by the temperature inversion layer in the Tianshan Mountains (Guo and Li, 2015). This elevation dependence pattern was in consistent with the elevation dependence in precipitation wetting trend in a previous study (Xu et al., 2018).

4.3. Uncertainty of reconstructed snow depth

The results of reconstructed snow depth exhibited overestimation in spring and autumn, but underestimation in winter, and the uncertainties of reconstructed snow depth were larger at high altitude regions. The uncertainty could be ascribed to three reasons: the uncertainty of reanalysis datasets, the uncertainty of ANN models, and other factors that caused change in snow depth.

The reanalysis reliability can vary substantially depending on factors such as the location and time period. For example, the strong spatial heterogeneity in precipitation and large topographical gradient in the study area make it challenging to evaluate gridded precipitation quantities using *in-situ* measurements. This is not only due to the scarcity of stations, but also the representation of *in-situ* observations. In addition, the evaluation of reanalysis and observations was only carried during the period of 1961 to 2014. This study assumed that the error between reanalysis data and observations remained the same during the past. Although it is unclear whether the error between reanalysis data and observations is the same during past and present, the uncertainty of reconstructed snow depth should reduce after bias correction.

The ANN model provides a mathematically valid, pattern recognition technique to produce complex algorithms describing the interrelationships among a number of input and output variables, and the model is useful for dealing with abundant data with non-linear and seasonal tendencies (Rumelhardt and McLelland, 1986). However, the ANN model cannot explain the physical dynamics in snow depth changes because it is a relative “black box” compared with the logistic regression model (Tu, 1996). This may reduce the confidence of the ANN models. In addition, the determination of proper ANN model structure is another factor that affects the accuracy of ANN models, implying that more calibration for ANN model structure is required. In this study, the best structure model for every station was selected among six models listed in Table 2 by comparing the errors between results and observations. More ANN models with different architectures applied for evaluating results will improve the accuracy and reduce the uncertainty. Moreover, the snow models that are based on the snowmelt process with thermodynamic mechanisms should be taken into account in future studies.

The change in snow depth is also affected by other factors apart from temperature and precipitation, such as blowing snow and metamorphism in snow and sublimation. Blowing snow is a typical event in mountain areas and triggers the redistribution of snow, especially at high altitudes (Groisman et al., 1991; Schmidt, 1982). This redistribution may contribute to the change in snow depth. When snow accumulation begins on the ground, the metamorphism in snow occurs. Soil temperature is the main thermal driver of snow metamorphism in winter. The bottom of the snowpack is warmer than the top, leading to

a large vertical temperature gradient causing recrystallization. According to a previous study, the vertical temperature from bottom to top was −0.15 °C to −0.5 °C in a snow profile in the Tianshan station for snow and avalanche research located in the Yili River Valley of the western Tianshan Mountains (Wang, 1982). Such metamorphism caused by great temperature gradient in snowpack also creates a change in snow depth. In addition, snow could be directly lost by sublimation in dry areas. Some studies have reported that sublimation loss could account for 30–51% of precipitation in winter (Berg, 1986). For an extreme instance, it reached a significant proportion at 50–80% of the total snowpack in the spring in the White Mountains of California (Beaty, 1975). A large amount of blowing snow can directly sublimate, causing a variation in snow depth (Donald, 1995; Liston, 2002). Note that these processes, such as blowing snow and sublimation, are not independent. The accumulation and ablation of snow are therefore complex processes, with complex energy and mass exchanges.

5. Conclusions

This study aimed to provide a flexible approach to reconstruct snow depth and extend it back to 1901 from 1960 based on reanalysis dataset. The results showed that the reconstructed snow depth using the ANN method is suitable for capturing the characteristic of snow depth. The response of snow depth to climate change was not consistent at different temporal and spatial scales. For temporal scale, increases of snow depth were revealed in southern and eastern Tianshan Mountains during the periods of 1901–1960, 1961–2014, and 1901–2014, respectively. However, the trends of snow depth indicated an increase in western, northern and overall Tianshan Mountains during periods of 1901–1960 and 1961–2014, but decreased during the overall 1901–2014 period. For spatial scale, higher values of snow depth occurred in the western and the northern regions, while the lower ones appeared in the southern and the eastern regions. In addition, the increasing trend in reconstructed snow depth was more profound with the increased elevation in the Tianshan Mountains during 1901–1960, with the smallest increasing rate at the elevation of 1000 m–1500 m. This study provides both a method for snow depth reconstruction and a dataset for the data deficient areas, which could be used in model simulation and future projection for comparison and evaluation. It also allows us to have a better understanding of regional climate change. Future studies will focus on the snow depth reconstruction applied by dynamic downscaling method which takes topographic factors into considerations.

Acknowledgments

This study was supported by the Strategic Priority Research Program of Chinese Academy of Sciences, Pan-Third Pole Environment Study for a Green Silk Road (Pan-TPE) (No. XDA2004030202) and the projects of National Natural Science Foundation of China (NSFC Grant U1703241, 41401030). Authors acknowledged a support from State Key Laboratory of Desert and Oasis Ecology. We are grateful to the supports from the Tianshan Station for Snow cover and Avalanche Research, Chinese Academy of Sciences, for data collection and analysis. The authors thank Dr. L. X. Li from Ontario Veterinary Medical Association for her linguistic assistance during the major revision of this manuscript.

The support for the Twentieth Century Reanalysis Project version 2c dataset is provided by the U.S. Department of Energy, Office of Science Biological and Environmental Research (BER), and by the National Oceanic and Atmospheric Administration Climate Program Office.

References

Aizen, V.B., Aizen, E.M., Melack, J.M., 1995. Climate, Snow Cover, Glaciers, and Runoff in the Tien Shan. Central Asia. J. Am. Water Resour. Assoc. 31, 1113–1129. https://doi.org/10.1111/j.1752-1688.1995.tb03426.x.

Barnett, J.C., Adam, D.P., Lettenmaier, T.P., 2005. Potential impacts of a warming climate on water availability in snow-dominated regions. Nature 438, 7.

Beaty, C.B., 1975. Sublimation or melting: observations from the White Mountains, California and Nevada. USA. J. Glaciol. 71, 275–286.

Berg, N.H., 1986. Blowing snow at a Colorado alpine site: measurements and implications. Arct. Alp. Res. 18 (2), 147–161.

Brown, R., Derksen, C., Wang, L., 2010. A multi-data set analysis of variability and change in Arctic spring snow cover extent, 1967-2008. J. Geophys. Res. 115. https://doi.org/10.1029/2010JD013975.

Bulygina, O.N., Razuvaev, V.N., Korshunova, N.N., 2011. Changes in snow cover over Northern Eurasia in the last few decades. Environ. Res. Lett. 6, 045026. https://doi.org/10.1088/1748-9326/4/4/045204.

Chen, J., Brissette, F.P., Leconte, R., 2011. Uncertainty of downscaling method in quantifying the impact of climate change on hydrology. J. Hydrol. 401, 190–202. https://doi.org/10.1016/j.jhydrol.2011.02.020.

Chen, J., St-Denis, B.G., Brissette, F.P., Lucas-Picher, P., 2016. Using Natural Variability as a Baseline to Evaluate the Performance of Bias Correction Methods in Hydrological climate Change Impact Studies. J. Hydrometeorol. 17, 2155–2174. https://doi.org/10.1175/JHM-D-15-0099.1.

Christensen, J.H., Boberg, F., Christensen, O.B., Lucas-Picher, P., 2008. On the need for bias correction of regional climate change projections of temperature and precipitation. Geophys. Res. Lett. 35, L20709. https://doi.org/10.1029/2008GL035694.

Compo, G.P., Whitaker, J.S., Sardeshmukh, P.D., Matsui, N., Allan, R.J., Yin, X., Gleason, E., Vose, R.S., Rutledge, G., Bessemoulin, P., Br, S., Marshall, G.J., Maugeri, M., Mok, H.Y., Nordli, Ø., Ross, T.F., Trigo, R.M., Wang, X.L., Woodruff, S.D., Worley, S.J., Weather, A., Africa, S., 2011. The Twentieth Century Reanalysis Project 1–28. https://doi.org/10.1002/qj.776.

Dobreva, I.D., Klein, A.G., 2011. Remote Sensing of Environment Fractional snow cover mapping through arti fi cial neural network analysis of MODIS surface reflectance. Remote Sens. Environ. 115, 3355–3366. https://doi.org/10.1016/j.rse.2011.07.018.

Donald, J.R., 1995. A land cover-based snow cover representation for distributed hydrologic models ploughed. Water Resour. Res. 31, 995–1009.

Dou, Y., Chen, X., 2010. A Study of the Snow Factors Temporal and Spatial Variation in the Tianshan Mountains based on Weather Stations Data. Adv. in Earth Sci. 26 (4), 441–448 (In Chinese).

Dyer, J.L., Mote, T.L., 2006. Spatial variability and trends in observed snow depth over North America. Geophys. Res. Lett. 33, 1–6. https://doi.org/10.1029/2006GL027258.

Groisman, P.Y., Koknaeva, V.V., Belokrylova, T.A., Karl, T.R., 1991. Overcoming Biases of Precipitation Measurement: A History of the USSR Experience. Bull. Am. Meteorol. Soc. https://doi.org/10.1175/1520-0477(1991)072<1725:OBOPMA>2.0.CO;2.

Guo, L., Li, L., 2015. Variation of the proportion of precipitation occurring as snow in the Tian Shan Mountains, China. Int. J. Climatol. 35, 1379–1393. https://doi.org/10.1002/joc.4063.

Hagemann, S., Chen, C., Haerter, J.O., Heinke, J., Gerten, D., Piani, C., 2011. Impact of a Statistical Bias Correction on the projected Hydrological changes Obtained from three GCMs and two Hydrology Models. J. Hydrometeorol. 12, 556–578. https://doi.org/10.1175/2011JHM1336.1.

Hartmann, D.J., Klein Tank, A.M.G., Rusticucci, M., Alexander, L.V., Brönnimann, S., Charabi, Y.A.-R., Dentener, F.J., Dlugokencky, E.J., Easterling, D.R., Kaplan, A., Soden, B.J., Thorne, P.W., Wild, M., Zhai, P., 2013. Observations: Atmosphere and Surface. Clim. Change 159–254. https://doi.org/10.1017/CBO9781107415324.008.

Hsu, K., Gupta, H.V., 1995. Artificial neural network modeling of the rainfall-runoff process that arise and based Background and Scope. Water Resour. Res. 31, 2517–2530.

Hu, R.J., 2004. Physical Geography of the Tianshan Mountains in China. China Environmental Science Press, pp. 443 (In Chinese).

Imrie, C.E., Durucan, S., Korre, A., 2000. Riverflow prediction using arti ficial neural networks: generalisation beyond the calibration range. J. Hydrol. 233, 138–153.

Johnson, F., Sharma, A., 2011. Accounting for interannual variability : a comparison of options for water resources climate change impact assessments. Water Resour. Res. 47. https://doi.org/10.1029/2010WR009272.

Lenderink, G., Buishand, A., Van Deursen, W., 2007. Estimates of future discharges of the river Rhine using two scenario methodologies : direct versus delta approach. Hydrol. Earth Syst. Sci. 11, 1145–1159.

Li, L., Simonovic, S.P., 2002. System dynamics model for predicting floods from snowmelt in north American prairie watersheds. Hydrol. Process. 16, 2645–2666. https://doi.org/10.1002/hyp.1064.

Li, X., Li, L., Wang, X., Jiang, F., 2013. Reconstruction of hydrometeorological time series and its uncertainties for the Kaidu River Basin using multiple data sources. Theor. Appl. Climatol. 113, 45–62. https://doi.org/10.1007/s00704-012-0771-2.

Li, B., Chen, Y., Chen, Z., Xiong, H., Lian, L., 2016. Why does precipitation in Northwest China show a significant increasing trend from 1960 to 2010? Atmos. Res. 167, 275–284. https://doi.org/10.1016/j.atmosres.2015.08.017.

Liston, G., 2002. Winter Precipitation patterns in Arctic Alaska Determined from a Blowing-Snow Model and Snow-Depth Observations. J. Hydrometeorol. 3, 646–659.

Ma, L., Qin, D., 2012. Temporal-spatial characteristics of observed key parameters of snow cover in China during 1957 – 2009. J. Glaciol. Geocryol. 4, 384–393. https://doi.org/10.3724/SP.J.1226.2012.00384.

Moghim, S., Bras, R.L., 2017. Bias Correction of climate Modeled Temperature and Precipitation using Artificial Neural Networks. J. Hydrometeorol. 18, 1867–1884. https://doi.org/10.1175/JHM-D-16-0247.1.

Qin, D.H., Liu, S.Y., Li, P.J., 2006. Snow cover distribution, variability, and response to climate change in western. China. J. Clim. 19, 1820–1833. https://doi.org/10.1175/JCLI3694.1.

Qiu, J., Sun, X., 1992. Preliminary study on snow cover in the Tianshan Mountains. Arid Land Geogr. 9–21 (In Chinese).
Reyers, M., Pinto, J.G., Paeth, H., 2013. Statistical-dynamical downscaling of present day and future precipitation regimes in the Aksu river catchment in Central Asia. Glob. Planet. Change 107, 36–49. https://doi.org/10.1016/j.gloplacha.2013.04.003.
Rumelhardt, D.E., McLelland, J.L., 1986. Parallel Distributed Processing Explorations in the Microstructure of Cognition. MIT Press, Cambridge, MA.
Schmidli, J., Frei, C., Vidale, P.L., 2006. Downscaling from GCM precipitation : a benchmark. Int. J. Climatol. 689, 679–689. https://doi.org/10.1002/joc.1287.
Schmidt, R., 1982. Properties of Blowing Snow. Rev. Geophys. 20, 39–44.
Shi, Y., Shen, Y., Kang, E., Li, D., Ding, Y., Zhang, G., Hu, R., 2007. Recent and future climate change in Northwest China. Clim. Chang. 80, 379–393. https://doi.org/10.1007/s10584-006-9121-7.
Tang, Z., Wang, X., Wang, J., Wang, X., Li, H., Jiang, Z., 2017. Spatiotemporal Variation of Snow Cover in Tianshan Mountains, Central Asia, based on Cloud-Free MODIS Fractional Snow Cover Product, 2001–2015. Remote Sens. 9, 2001–2015. https://doi.org/10.3390/rs9101045.
Tedesco, M., Pulliainen, J., Takala, M., Hallikainen, M., Pampaloni, P., 2004. Artificial neural network-based techniques for the retrieval of SWE and snow depth from SSM / I data. Remote Sens. Environ. 90, 76–85. https://doi.org/10.1016/j.rse.2003.12.002.
Teutschbein, C., Seibert, J., 2012. Bias correction of regional climate model simulations for hydrological climate-change impact studies : Review and evaluation of different methods. J. Hydrol. 456–457, 12–29.
Tu, J.V., 1996. Advantages and disadvantages of using artificial neural networks versus logistic regression for predicting medical outcomes. J. Clin. Epidemiol. 49, 1225–1231.
Wang, Y., 1982. Metamophism of seasonal snow cover in the upper reaches of Ylihe in Tianshan. J. Glaciol. Cryopedol. 4, 63–72 (In Chinese).
Wang, Q., Wei, W., Wang, J., 2008. Temporal variation of the maximum snow cover depth in North Xinjiang derive from EOF. J. Glaciol. Geocryol. 30, 244–249 (In Chinese).
Wei, N., Gong, Y., Sun, X., Fang, J., 2005. 2010: Variation of precipitation and water vapor transpot over the Northwest China from 1959 to. J. Desert Res. 30, 1450–1457 (In Chinese).
Widmann, M., Bretherton, C., Salathe, J.R., 2003. Statistical Precipitation Downscaling over the Northwestern United States using Numerically simulated Precipitation as a Predictor. J. Clim. 799–816.
Xu, W., Ma, L., Ma, M., Zhang, H., Yuan, W., 2017. Spatial-temporal variability of snow cover and depth in the Qinghai-Tibetan plateau. J. Clim. 30, 1521–1533. https://doi.org/10.1175/JCLI-D-15-0732.1.
Xu, M., Kang, S., Wu, H., Yuan, X., 2018. Detection of spatio-temporal variability of air temperature and precipitation based on long-term meteorological station observations over Tianshan Mountains. Central Asia. Atmos. Res. 203, 141–163. https://doi.org/10.1016/j.atmosres.2017.12.007.
Yang, Q., 2008. Snow Cover Variation in the past 45 years (1959-2003) in the Tianshan Mountains. China. Adv. Clim. Chang. Res. 4, 13–17.
Yao, J., Yang, Q., Mao, W., Zhao, Y., Xu, X., 2016. Precipitation trend-Elevation relationship in arid regions of the China. Glob. Planet. Change 143, 1–9. https://doi.org/10.1016/j.gloplacha.2016.05.007.
Ye, H., Ellison, M., 2003. Changes in transitional snowfall season length in northern Eurasia. Geophys. Res. Lett. 30, 94–96. https://doi.org/10.1029/2003GL016873.
Yu, Y., Wang, J., Li, Q., 2003. Spatial and temporal distribution of water vapor and its variation trend in atmosphere over Northwest China. J. Glaciol. Geocryol. 25, 149–156 (in Chinese).
Zhang, F., Ahmad, S., Zhang, H., Zhao, X., Feng, X., Li, L., 2016a. Simulating low and high streamflow driven by snowmelt in an insufficiently gauged alpine basin. Stoch. Environ. Res. Risk Assess. 30, 59–75. https://doi.org/10.1007/s00477-015-1028-2.
Zhang, F., Bai, L., Li, L., Wang, Q., 2016b. Sensitivity of runoff to climatic variability in the northern and southern slopes of the Middle Tianshan Mountains. China. J. Arid Land 8, 681–693. https://doi.org/10.1007/s40333-016-0015-x.
Zhou, H., Aizen, E., Aizen, V., 2017. Seasonal snow cover regime and historical change in Central Asia from 1986 to 2008. Glob. Planet. Change 148, 192–216.